Impact of PsbTc on Forward and Back Electron Flow, Assembly, and Phosphorylation Patterns of Photosystem II in Tobacco[1[W][OA]]

Pavan Umate[2,3], Christine Fellerer[2], Serena Schwenkert, Mikael Zoryan, Lutz A. Eichacker, Abbagani Sadanandam, Itzhak Ohad, Reinhold G. Herrmann, and Jörg Meurer*

Department of Biology I, Botany, Ludwig-Maximilians-University Munich, 80638 Munich, Germany (P.U., C.F., S.S., M.Z., L.A.E., R.G.H., J.M.); Department of Botany, Kakatiya University, Warangal 506 009, India (A.S.); and Department of Biological Chemistry and Minerva Center of Photosynthesis Research, Hebrew University of Jerusalem, Jerusalem 91904, Israel (I.O.)

Photosystem II (PSII) of oxygen-evolving cyanobacteria, algae, and land plants mediates electron transfer from the Mn_4Ca cluster to the plastoquinone pool. It is a dimeric supramolecular complex comprising more than 30 subunits per monomer, of which 16 are bitopic or peripheral, low-molecular-weight components. Directed inactivation of the plastid gene encoding the low-molecular-weight peptide PsbTc in tobacco (*Nicotiana tabacum*) does not prevent photoautotrophic growth. Mutant plants appear normal green, and levels of PSII proteins are not affected. Yet, PSII-dependent electron transport, stability of PSII dimers, and assembly of PSII light-harvesting complexes (LHCII) are significantly impaired. PSII light sensitivity is moderately increased and recovery from photoinhibition is delayed, leading to faster D1 degradation in Δ*psb*Tc under high light. Thermoluminescence emission measurements revealed alterations of midpoint potentials of primary/secondary electron-accepting plastoquinone of PSII interaction. Only traces of CP43 and no D1/D2 proteins are phosphorylated, presumably due to structural changes of PSII in Δ*psb*Tc. In striking contrast to the wild type, LHCII in the mutant is phosphorylated in darkness, consistent with its association with PSI, indicating an increased pool of reduced plastoquinone in the dark. Finally, our data suggest that the secondary electron-accepting plastoquinone of PSII site, the properties of which are altered in Δ*psb*Tc, is required for oxidation of reduced plastoquinone in darkness in an oxygen-dependent manner. These data present novel aspects of plastoquinone redox regulation, chlororespiration, and redox control of LHCII phosphorylation.

PSII, the oxygen-evolving pigment-protein complex of the thylakoid membrane system, is present in photosynthetic organisms from cyanobacteria to vascular plants. The proteins of the photochemically active reaction center (RC), the heterodimeric polypeptides PsbA (D1) and PsbD (D2) and the low-molecular-weight (LMW) subunits PsbE and PsbF, and the α- and β-chains of cytochrome b_{559} coordinate the redox cofactors necessary for primary PSII photochemistry. Electron flow following charge separation occurs via several electron carriers of the RC, including pheophytin *a*, as well as the primary and secondary quinones, Q_A and Q_B. The striking similarities between cyanobacterial and land plant PSII core components, including the intrinsic light-harvesting antennae, the chlorophyll-binding proteins CP43 and CP47, and their interactions during photosynthetic charge separation, suggest a high degree of structural and functional conservation. Thus, much of the information obtained from crystallization of a cyanobacterial PSII can be applied to that of higher plants (Zouni et al., 2001; Kamiya and Shen, 2003; Ferreira et al., 2004; Loll et al., 2005; Nield and Barber, 2006).

Besides the RC, the PSII core contains a remarkably high number (16) of intrinsic or peripheral LMW peptides. Five of them are encoded in eukaryotes by nuclear genes (*psb*R, *psb*Tn, *psb*W, *psb*X, and *psb*Y1/*psb*Y2) and 11 by plastid genes (*psb*E, *psb*F, *psb*L, *psb*J, *psb*K, *psb*M, *psb*I, *psb*Tc, *psb*N, *psb*H, and *psb*Z), of which most are parts of conserved operons (for review, see Minagawa and Takahashi, 2004; Shi and Schröder, 2004; Thornton et al., 2005; Müh et al., 2008). PSII cores of higher plants and cyanobacteria form a functional dimer. In chlorophyll *a*/*b* lineages, the additional chlorophyll proteins light-harvesting complex II (LHCII),

[1] This work was supported by the Deutsche Forschungsgemeinschaft (grant no. SFB–TR1 to J.M. and R.G.H.), the Deutsche Akademische Austauschdienst (to P.U.), and the Minerva Avron, Even-Ari Center for Photosynthesis Research, Hebrew University, Jerusalem, Israel (to I.O.).

[2] These authors contributed equally to the article.

[3] Present address: Plant Molecular Biology, International Centre for Genetic Engineering and Biotechnology, Aruna Asaf Ali Marg, New Delhi 110 067, India.

* Corresponding author; e-mail joerg.meurer@lrz.uni-muenchen.de.

The author responsible for distribution of materials integral to the findings presented in this article in accordance with the policy described in the Instructions for Authors (www.plantphysiol.org) is: Jörg Meurer (joerg.meurer@lrz.uni-muenchen.de).

[W] The online version of this article contains Web-only data.

[OA] Open Access articles can be viewed online without a subscription.

www.plantphysiol.org/cgi/doi/10.1104/pp.108.126060

forming trimers CP24, CP26, and CP29, are associated with dimeric PSII complexes and, except for CP24, partially with PSI, depending on the energy balance between the two photosystems (Dekker and Boekema, 2005; Takahashi et al., 2006). This process is regulated by reversible phosphorylation of these chlorophyll-binding proteins. Excess light excitation of PSII relative to the accessibility of the electron sink induces back electron flow and charge recombination that generates singlet oxygen species, considered one of the causes of photoinactivation and related light-dependent degradation of the D1 protein (Vass et al., 2007) as well as of a genetically programmed stress response (Wagner et al., 2004). Another primary event of photodamage to PSII may be a direct inactivation of the oxygen-evolving complex (Hakala et al., 2005; Ohnishi et al., 2005).

The conservation of PSII LMW peptides throughout evolution from cyanobacteria to plastids suggests that those proteins that are not harboring any of the electron carrier components play distinct roles in the structural organization, dynamics, and regulation of PSII electron flow and its protein turnover. Possible roles for the LMW peptides in these processes have been discussed for cyanobacteria, algae, and land plants (Minagawa and Takahashi, 2004; Shi and Schröeder, 2004; Thornton et al., 2005; Müh et al., 2008). In this context, it is relevant to mention that inactivation of some of these genes often resulted in different phenotypes in distantly related organisms (Regel et al., 2001; Ohad et al., 2004; Schwenkert et al., 2006). Detailed analyses of knockout mutants of PSII LMW peptides in tobacco (*Nicotiana tabacum*) have revealed specific roles for PsbE, PsbF, PsbL, and PsbJ (Regel et al., 2001; Swiatek et al., 2003b; Ohad et al., 2004) as well as for PsbZ (Swiatek et al., 2001), PsbI (Schwenkert et al., 2006), and PsbM (Umate et al., 2007).

Two different LMW peptides associated with PSII were originally designated PsbT. PsbTc of 4 kD originates from a chloroplast gene, and the unrelated protein PsbTn of 11 kD originates from a nuclear gene (for review, see Shi and Schröder, 2004; Müh et al., 2008). PsbTc is an intrinsic, bitopic LMW protein harboring a single transmembrane helix and, different from most LMW peptides, exposes its N-terminal tail to the lumenal phase of the thylakoid membrane (Shi and Schröder, 2004). The *psb*Tc gene is located in a highly conserved operon, together with the PSII genes *psb*B and *psb*H, the cytochrome b_6f complex genes *pet*B and *pet*D, encoding cytochrome b_6 and subunit IV, and *psb*N on the opposite strand. The operon is transcribed into a primary product of 5.7 kb that is processed in a complex way (Barkan, 1988; Kohchi et al., 1988; Westhoff and Herrmann, 1988).

As part of an ongoing project, individual thylakoid LMW peptides were systematically disrupted in tobacco to elucidate the effect of each in the same organism. Here, the first study (to our knowledge) of the effect of *psb*Tc inactivation on PSII function in a higher plant is presented. Our data show that Q_A and Q_B site properties, forward and back electron flow, phosphorylation, assembly, and stability of PSII proteins are affected in the mutant. In addition, experiments performed with the wild type reveal that in vivo the Q_B site of PSII is responsible for the oxidation of reduced plastoquinone and the reduction of oxygen in the dark, presumably to keep the acceptor side of PSII oxidized. This sheds new light on the nature of a terminal oxidase working during chlororespiration.

RESULTS

Inactivation of *psb*Tc

To selectively inactivate *psb*Tc, we inserted a terminatorless amino glycoside 3′ adenyl transferase (*aad*A) cassette into a newly introduced restriction site in the 5′ region of the gene to avoid expression of a functional or truncated protein (Fig. 1A). Homoplastomy of transformed lines was confirmed by PCR analysis of isolated chloroplast chromosomes (Fig. 1B). Primers used for PCR did not amplify the 1,021-bp product obtained for the wild type but exclusively amplified the *aad*A-containing product of 1,952 bp in Δ*psb*Tc. Insertion of the selection cassette into a pentacistronic operon could affect the expression, processing, and/or stability of transcripts originating from the same operon or, in this case, from the oppositely transcribed *psb*N. Therefore, the integrity and levels of well-known processed RNA species (Westhoff and Herrmann, 1988) were estimated by northern-blot analyses using strand-specific probes for *psb*Tc, *psb*H, and *psb*N as well as random primed labeled probes for *psb*B and *pet*B (Fig. 1C). These data confirmed the homoplastomic state of mutant plants, since spliced and unspliced pentacistronic transcripts, detected with *psb*B, *psb*Tc, *psb*H, and *pet*B probes, as well as dicistronic *psb*B-*psb*T transcripts, are expectedly up-shifted by the size of the *aad*A cassette. Although no monocistronic *psb*Tc transcripts could be detected in the wild type, the *psb*B-*psb*Tc intergenic region was processed in the mutant, resulting in the accumulation of a *psb*Tc-*aad*A transcript of about 1.3 kb. The analysis further demonstrated that processing and expression levels of *psb*H-, *psb*N-, and *pet*B-containing transcripts located downstream of *psb*Tc are not notably affected by the *aad*A insertion (Fig. 1C). Mutant plants grew photoautotropically under greenhouse conditions on soil and appeared green, comparable to wild-type plants. In contrast to the wild type, PsbTc could not be detected in mutant thylakoid membranes by mass spectrometry using a novel approach, which will be published elsewhere (Granvogl et al., 2008). To ensure that the phenotype was not caused by random nuclear background mutations and inherited solely via chloroplasts, we performed backcrosses with the wild type using three independently generated homoplastomic Δ*psb*Tc mutants as female parents. This resulted in a 100% offspring of the mutant phenotype with respect

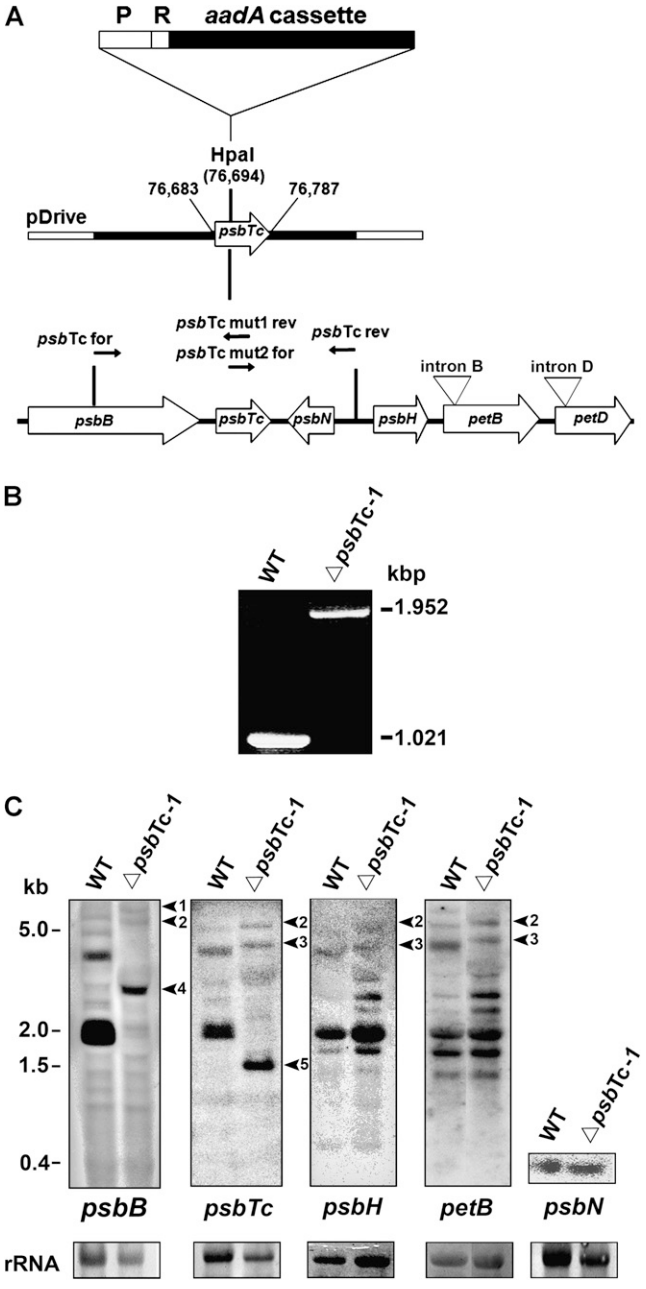

Figure 1. A, Strategy for inactivation of the chloroplast *psb*Tc gene. The organization of the *psb*B operon with the genes *psb*B, *psb*Tc, *psb*H, *pet*B, *pet*D, and *psb*N on the opposite strand is indicated. Arrows designate the direction of their transcription. The *aad*A selection cassette without termination signal and its 16S rDNA promoter (P) and ribosome-binding site (R) were inserted into the introduced *Hpa*I restriction site (plastome position 76,694 bp) of the *psb*Tc coding frame (plastome position 76,683–76,787 bp). B, PCR products of the *psb*Tc region in the wild type (WT) and mutant indicate the homoplastomic state of the insertion. C, Northern analysis of the wild type and Δ*psb*Tc-1 using double-strand (*pet*B and *psb*B) and single-strand (*psb*Tc, *psb*H, and *psb*N) probes. Arrowheads indicate shifted *psb*Tc-containing transcripts, confirming the homoplastomic state of the *aad*A insertion. Arrowheads 1 to 3 correspond to the up-shifted *aad*A containing primary spliced and unspliced transcripts in Δ*psb*Tc-1. Arrows 4 and 5 indicate the up-shifted *psb*B-*psb*Tc-*aad*A and the appearing *psb*Tc-*aad*A transcript in the mutant, respectively. Ribosomal RNA (rRNA) was stained with methylene blue as a loading control.

to photosynthetic parameters, such as reduction of the potential maximum quantum yield of PSII (F_v/F_m), to about 0.68 ± 0.03 compared with 0.82 ± 0.01 in the wild type using at least 20 individuals from each cross. This unequivocally indicates that loss of PsbTc accounts exclusively for the phenotype. Three chosen mutant lines, Δ*psb*Tc-1 to -3, were used for detailed studies.

Composition of Thylakoid Membrane Proteins in Δ*psb*Tc-1

The protein composition of thylakoids isolated from Δ*psb*Tc and wild-type plants was estimated by immunoblot analysis using antisera raised against individual thylakoid proteins (Schwenkert et al., 2006). Levels of PSII proteins D1, D2, CP47, and PsbI and the extrinsic polypeptide PsbO of the oxygen-evolving complex in Δ*psb*Tc-1 were comparable with those of the wild type (Fig. 2A). Also, no notable differences were found for the major LHCII (Lhcb1), LHCI (Lhca1), and minor antenna apoproteins CP29, CP26, and CP24 or for components of PSI, the cytochrome b_6f complex, and ATP synthase (Fig. 2A; data not shown). This corroborates that translation and accumulation of *pet*B and *pet*D transcripts downstream of *psb*Tc-1 are not affected by the *aad*A insertion.

Assembly of PSII-LHCII Supercomplexes and Stability of PSII Dimers Are Affected in Δ*psb*Tc-1 to -3

To gain information on the assembly and stability of PSII in Δ*psb*Tc plants, controlled partial lysates of isolated thylakoids solubilized with 1% β-dodecylmaltoside were resolved by blue native (BN)-PAGE and subsequent SDS-PAGE. The protein patterns uncovered that PSII-LHCII supercomplexes were almost missing and levels of dimeric PSII complexes were reduced, whereas trimeric LHCII complexes, as well as monomeric PSII RC complexes lacking CP43, called RC47, were increased in Δ*psb*Tc-1 to -3 thylakoids compared with the wild type (Fig. 2B; Supplemental Fig. S1A). Levels and sizes of all other detectable thylakoid membrane complexes were not significantly affected. To estimate a possible loss of unstable PSII supercomplexes in the mutant during sample preparation, milder separation of thylakoid lysates by Suc density gradient centrifugation and BN-PAGE using 1.5% digitonin (Schwenkert et al., 2007) was applied. Separation profiles confirmed reduced levels of PSII-LHCII supercomplexes in the mutant (Supplemental Fig. S2, A and B). Levels of monomeric RC47 complexes and trimeric LHCII complexes were increased in Δ*psb*Tc-1 (Supplemental Fig. S2, A and B), suggesting that assembly and/or stability of higher order PSII complexes are affected or that they could not be

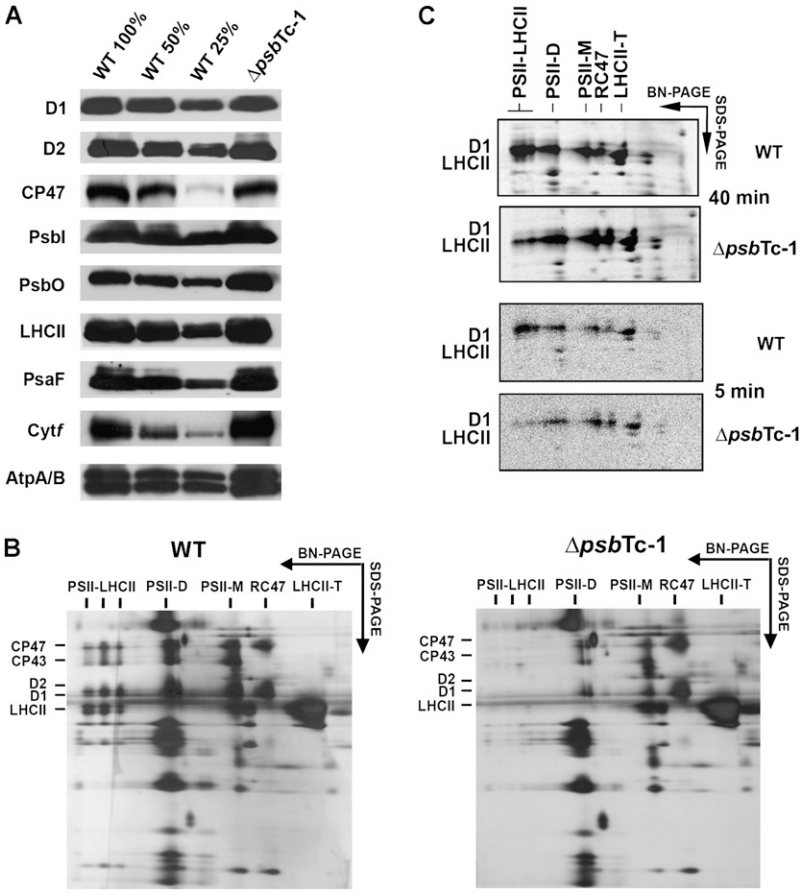

Figure 2. A, Western-blot analysis of wild-type (WT) and Δ*psb*Tc-1 thylakoid proteins. The designation 100% corresponds to 5 μg of chlorophyll. B, Separation of wild-type and Δ*psb*Tc-1 thylakoid protein complexes by BN-SDS-PAGE. Complexes and silver-stained proteins are labeled according to their identification by mass spectrometry. Comparable results were obtained from two further independently generated mutant plants (Supplemental Fig. S1A). D, Dimer; M, monomer; T, trimer. Note that PSII-LHCII supercomplexes are lacking and levels of PSII dimers are reduced. C, Autoradiograph of in vivo radiolabeled thylakoid membrane protein complexes separated by BN-PAGE and SDS-PAGE. Intact leaves labeled for 40 and 5 min showed impaired assembly of PSII-LHCII supercomplexes, whereas dimer assembly was not affected in Δ*psb*Tc-1.

readily isolated in Δ*psb*Tc thylakoids. Therefore, a third approach was chosen to discern whether the formation or stability of PSII-LHCII supercomplexes and dimeric complexes is affected in Δ*psb*Tc-1. Leaves were labeled with [^{35}S]Met, and isolated thylakoids were analyzed by two-dimensional BN-SDS-PAGE (Fig. 2C). This approach showed that the mutant is capable of assembling RC47, PSII monomers, and dimers efficiently but not PSII-LHCII supercomplexes compared with the wild type. Since steady-state levels of dimers are severely reduced, we conclude that the stability of dimeric PSII complexes is affected by the mutation, presumably due to conformational changes induced by the absence of PsbTc. The relative amount of assembled PSII-LHCII complexes even after a short 5-min pulse resembles the pattern after a pulse of 40 min (Fig. 2C), indicating that the supercomplexes are not lost because of severe instability during the labeling period in Δ*psb*Tc-1. Improper assembly of LHCII may result secondarily from conformational changes of the PSII dimer (Fig. 2C).

Light Sensitivity: Photoinactivation and Recovery of PSII Activity

Upon excessive illumination, D1 protein is damaged and degraded, resulting in impaired PSII activity. Therefore, the extent of PSII light sensitivity and its ability to recover from photoinactivation were studied by measuring F_v/F_m as an estimation of the potential PSII quantum yield in wild-type and mutant plants. In order to distinguish between PSII damage and repair (de novo D1 synthesis) processes, the effect of the chloroplast protein synthesis inhibitor D-threo-chloramphenicol (CAP) was examined. For this, we chose saturating concentrations of CAP (200 μg mL^{-1}) in darkness and incubation times (30 min) sufficient to completely block D1 synthesis (Supplemental Fig. S1B). Wild-type and Δ*psb*Tc-1 to -3 leaf discs were illuminated at 1,200 μE m^{-2} s^{-1} after pretreatment with CAP. In the absence of CAP (control conditions), F_v/F_m was reduced to about 50% of the initial value in all three mutant lines compared with only 66% ± 1.2% in the wild type after 4 h of illumination (Fig. 3A; Supplemental Fig. S1C). Addition of CAP induced a more pronounced PSII inactivation in both wild-type and Δ*psb*Tc-1 to -3 plants to 33% ± 1.3% and 20% to 23% of their initial values, respectively (Fig. 3A; Supplemental Fig. S1C). This shows that recovery principally takes place and that PSII is more sensitive to high light exposure in the mutants than in wild-type plants. To further analyze the efficiency of the recovery process, wild-type and Δ*psb*Tc-1 leaf disc samples were exposed to 1,200 μE m^{-2} s^{-1} until the PSII quantum

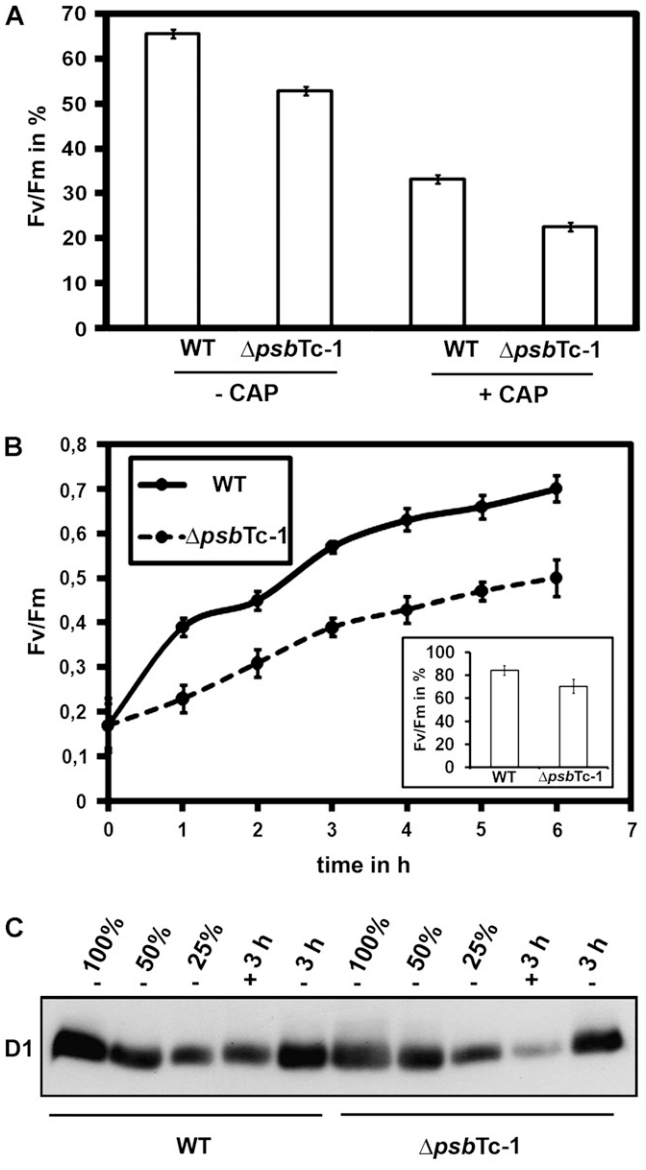

Figure 3. Photoinhibition of PSII and recovery kinetics of high light-treated wild-type (WT) and mutant leaves. A, Loss of quantum yield (F_v/F_m) with and without CAP after exposition to 1,200 μE m^{-2} s^{-1} for 4 h. F_v/F_m ratios are expressed relative to the initial values before starting the experiment in the wild type (F_v/F_m approximately 0.82) and mutants (F_v/F_m approximately 0.68), respectively (see data for independent transformants in Supplemental Fig. S1C). B, PSII recovery from photoinhibition of wild-type and Δ*psb*Tc-1 mutant leaves exposed to photoinhibition at 1,200 μE m^{-2} s^{-1} until a F_v/F_m ratio of 0.17 was reached by each sample. PSII recovery was followed by further incubation of the samples at 3 μE m^{-2} s^{-1} for the times indicated. Total recovery after 6 h is depicted as the ratio F_v/F_m as a percentage of the original F_v/F_m in the wild type and mutant. Error bars in A and B represent SD of at least three independent experiments. C, Immunoblot analysis of the wild type and Δ*psb*Tc-1 with D1-specific antibodies before and 3 h after photoinhibition (3 h) at 1,200 μE m^{-2} s^{-1} with (+) and without (−) CAP. Five micrograms of chlorophyll was loaded, and equal loading was routinely checked either by immunoblot analysis with antibodies raised against cytochrome b_6 or by gel staining.

yield reached 0.17 in all samples and then were allowed to recover PSII activity under very low light intensity (3 μE m^{-2} s^{-1}; Fig. 3B). After 2 h, recovery was about two times faster in the wild type compared with Δ*psb*Tc-1. Mutant leaf samples finally recovered 70.4% ± 8% of their initial PSII activity compared with 84.2% ± 7% in the wild type within 6 h, indicating a delayed recovery of PSII activity from photoinhibition in Δ*psb*Tc-1. To further analyze photosensitivity at the protein level, quantitative immunological analysis with D1 proteins of high light-treated wild-type and mutant plants was performed in the absence and presence of CAP (Fig. 3C). We calculated that D1 accumulates to about 85% in the wild type and to 70% in the mutant at 3 h after photoinhibition. After CAP and high light treatment, D1 was reduced to approximately 45% in the wild type and to 15% in the mutant. These data confirmed that the photoinhibitory effect in Δ*psb*Tc-1 was indeed due to D1 degradation and that CAP induced a more pronounced degradation of D1 in the mutant compared with the wild type, again indicating an increased light sensitivity of PSII in Δ*psb*Tc-1 (Fig. 3C).

Activities of PSII and PSI

The maximum quantum yield of PSII, F_v/F_m, was decreased in all independently selected and backcrossed mutant lines (Δ*psb*Tc-1 to -3) and ranged from 0.65 to 0.71 versus 0.82 ± 0.01 in the wild type, which was due to an increased F_o and/or a decreased F_v, again indicating dissociation of the outer PSII antenna and/or malfunction of PSII electron transport activity. Further photosynthetic parameters have been measured in the three lines (Fig. 4). The photochemical quenching parameter (qP) as well as the effective PSII yield (Φ_{PSII}) were decreased at 5 and 45 μE m^{-2} s^{-1} red actinic light in Δ*psb*Tc-1 to -3 mutant plants (Fig. 4, A and C), indicating a partial loss of PSII function. Nonphotochemical quenching (NPQ) was also significantly lower at both light intensities, amounting to only about 50% in the mutants compared with the wild type at red light intensity of 45 μE m^{-2} s^{-1}, indicating a decreased transmembrane proton gradient due to lower PSII activity (Fig. 4B). The PSI oxidation state at 5 and 45 μE m^{-2} s^{-1} red light intensities was about 7-fold and 4-fold higher, respectively, in Δ*psb*Tc-1 to -3 compared with the wild type (Fig. 4D). Since NPQ is significantly decreased at both light intensities, the increased oxidation level of P700 can be solely attributed to a lower capacity of electron transfer from PSII to the plastoquinone pool in the mutants. This inference is supported by steady-state fluorescence measurements (F_s') elicited by 650-nm actinic light at an intensity of 34 μE m^{-2} s^{-1} on far-red background light (12 W m^{-2}). The ratio F_s' Δ*psb*Tc-1 to F_s' wild type was 0.77, illustrating that the rate of electron flow toward plastoquinone is lower than that from plastoquinol to the electron sink via PSI in the mutant. These results are also supported by a lowered PSII activity ranging

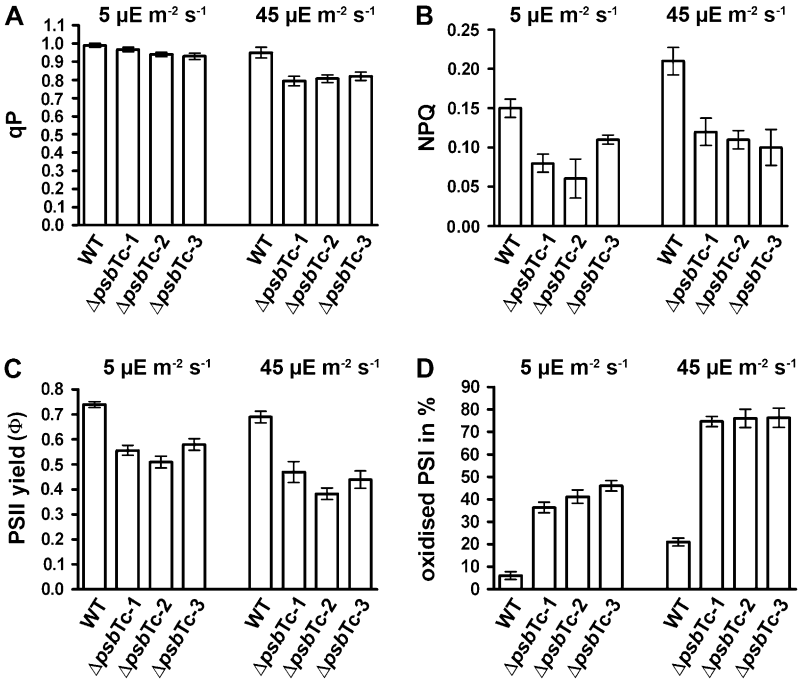

Figure 4. Photosynthetic performance in the wild type (WT) and the three mutant lines Δ*psb*Tc-1 to -3. Photosynthetic parameters, as indicated by qP (A), NPQ (B), Φ_{PSII} values (C), and P700 oxidation ratio measured as $\Delta A/\Delta A_{max}$ (D), were calculated from wild-type and mutant plants kept in the steady state at 5 and 45 μE m^{-2} s^{-1} red light intensities. Error bars represent SD of at least three independent experiments.

from 65% to 76% in three mutant plants compared with wild-type thylakoids, measured as oxygen evolution under saturating light conditions in the presence of uncouplers.

Electron Flow within PSII as Measured by Thermoluminescence

Thermoluminescence (TL) measurements were performed to further investigate the effect of *psb*Tc inactivation on electron flow within PSII. Activation energy required for back electron flow from Q_B^- to the $S_{2,3}$ states of the Mn_4Ca donor side of PSII via P_{680}^+ charge recombination is supplied by temperature rise and accompanied by light emission. The temperature at which recombination and light emission are maximal is related to the redox potential difference between the recombining charge-separated pairs and thus to the energy input required to drive the back electron flow (Krieger-Liszkay and Rutherford, 1998; Rutherford and Krieger-Liszkay, 2001). Charge recombination between Q_B^- and oxidized states of S_2 or S_3 occurs at about 35°C. The luminescence emission appearing at this temperature is designated the B band (Schwenkert et al., 2006; Ducruet et al., 2007). Blocking electron flow to the Q_B site results in back electron flow from Q_A^- and charge recombination with the $S_{2/3}$ state, resulting in the Q band emission. Due to the lower energy gap between these recombining pairs, the Q band temperature occurs at about 3°C to 5°C. This is the case when phenolic-type herbicides, such as Ioxynil, bind at the Q_B site (Krieger-Liszkay and Rutherford, 1998; Cser and Vass, 2007; Umate et al., 2007). However, binding of urea-type herbicides such as 3-(3,4-dichlorphenyl)-1,1-dimethylurea (DCMU) affects the Q_B site conformation and thus alters its interaction with the Q_A site, resulting in a decrease of the Q_A:Q_A^-/Q_B^-:Q_B redox potential gap and thus an up-shift of the required energy input to drive back electron flow that occurs at 12°C to 15°C (Krieger-Liszkay and Rutherford, 1998; Rutherford and Krieger-Liszkay, 2001; Ohad et al., 2004).

The B band emission temperature was up-shifted to about 38°C to 42°C (Fig. 5A), while the Q band temperature emitted in the presence of DCMU was strongly down-shifted to about 3°C in mutant thylakoids (Fig. 5A). The TL emission temperature in the presence of Ioxynil also showed a severe down-shift of the Q band emission temperature to −10°C in Δ*psb*Tc-1 and Δ*psb*Tc-2 (Fig. 5B). Strikingly, the concentration of Ioxynil (5 μM) that is sufficient to saturate the Q_B site in wild-type thylakoids, resulting only in emission of the Q band at 3°C, does not completely abolish the B band emission in the mutant, which shows an increase in the Q band and a decrease of the B band emission intensity with increasing Ioxynil concentration up to 20 μM (Fig. 5B). These results demonstrate that the absence of PsbTc induces significant conformational changes with respect to the Q_A and Q_B site properties.

The oxidation/reduction of the Mn_4Ca cluster usually occurs with a period of four stable steps (S_0–S_3) during oxygen evolution (Haumann et al., 2005), while that of the Q_B site occurs in two steps (Q_B and Q_B^-). Following transition from light to darkness, back electron flow from the reduced electron carriers of PSII (pheophytin$^-$, Q_A^-, and Q_B^-) occurs, resulting in the accumulation of about 25% S_0 and 75% S_1 states and a 1:1 ratio of Q_B^-/Q_B (Rutherford et al., 1982, 1984;

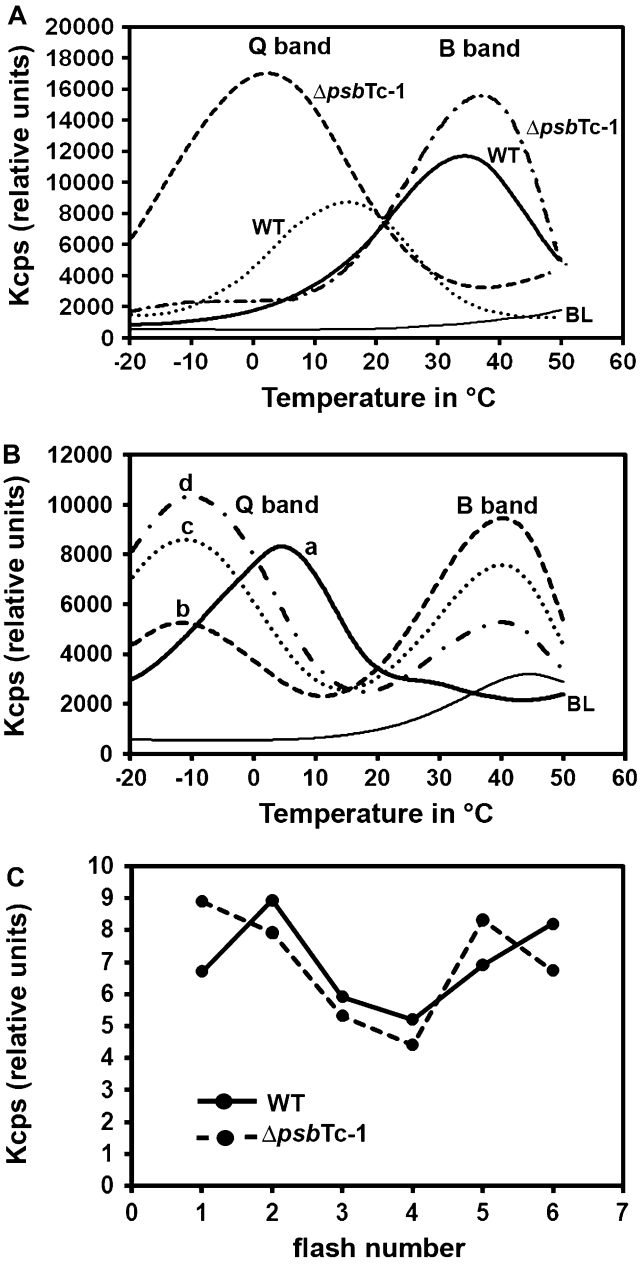

Figure 5. TL measurements of wild-type (WT) and Δ*psb*Tc-1 thylakoids. A, The B band occurring at 35°C in the wild type is slightly up-shifted to 38°C in the mutant. The Q band emission in the presence of DCMU (10 μM) occurs at 15°C in the wild type and at 3°C in Δ*psb*Tc. BL indicates the baseline signal generated from dark-adapted, unexcited samples. B, Q band emission of wild-type (a = 5 μM Ioxynil) and Δ*psb*Tc-1 (b = 5 μM, c = 10 μM, and d = 20 μM Ioxynil) thylakoid samples. The Q band emission temperature is down-shifted to −10°C at all Ioxynil concentrations compared with 3°C to 5°C in the wild type. Note that curves b, c, and d depict a persistent B band emission in the presence of Ioxynil. BL, Baseline. C, The B band oscillation pattern shows a 1/5 oscillation type in Δ*psb*Tc-1 compared with the typical 2/6 type for the wild type. All SD values are below 0.5%. Comparable results were obtained with Δ*psb*Tc-2 plants.

Krieger-Liszkay and Rutherford, 1998; Umate et al., 2007). The intensity of TL B band emission of dark-adapted tobacco thylakoids, following single-turnover excitations (one to six flashes), is proportional to the number of recombining $Q_B^-/S_{2,3}$ pairs and oscillates with the number of exciting single-turnover flashes with maximal emission at flashes 2 and 6 in the wild type (Umate et al., 2007). Since deletion of PsbTc shows drastic effects on the Q_A/Q_B site interactions and charge recombination, one would expect changes also in the oscillation pattern of the B band emission with the number of excitation flashes. Results of experiments addressing this question indeed showed an alteration of the TL B band oscillation patterns for Δ*psb*Tc-1 and Δ*psb*Tc-2, exhibiting emission maxima at flashes 1 and 5 (Fig. 5C). Using a simulation program for oscillation patterns (Umate et al., 2007), the ratio Q_B/Q_B^- present in dark-adapted thylakoids prior to the flash excitations was significantly increased in Δ*psb*Tc-1 (1.68 versus 0.90 in the wild type; Supplemental Table S1). These results support the conclusion that the back electron flow within PSII is altered in the mutant, presumably because of alterations of the Q_B binding site properties.

Effect of the Mutation on Redox-Controlled Phosphorylation of LHCII and PSII Core Proteins

Plants have developed several mechanisms to efficiently adjust their energy conversion to different light qualities and quantities. Shifting their antenna from one photosystem to the other (state transition) allows optimal adaptation to changing light conditions. Thus, phosphorylation and dephosphorylation of a mobile pool of CP29, CP26, and LHCII are induced under light, which preferentially excites PSII (state II) and PSI (state I), respectively (Rochaix, 2007). Regulation of phosphorylation of the D1, D2, and CP43 proteins is less understood. Therefore, phosphorylation and antenna association experiments were performed (Fig. 6, A and B). Strikingly, in the absence of PsbTc, the PSII core proteins D1/D2 were not phosphorylated and CP43 was only marginally phosphorylated under both state I and state II conditions in all three mutant lines (Fig. 6A; Supplemental Fig. S1D). On the other hand, in contrast to the wild type, LHCII was already highly phosphorylated in darkness and dephosphorylated under state II light conditions in Δ*psb*Tc-1 to -3. To check whether phosphorylation in the mutants results from a reduced plastoquinone pool in darkness, state I conditions were adjusted with far-red light. This light treatment abolished LHCII phosphorylation in both wild-type and mutant plants (Fig. 6A). Mild solubilization of thylakoids with digitonin and separation of lysates by BN-PAGE allows the detection of LHCII-PSI supercomplexes under state II light conditions in the wild type (Schwenkert et al., 2007). In contrast, in the mutant, LHCII-PSI supercomplexes were formed only in darkness, consistent with the phosphorylation pattern and the reduced state of the plastoquinone pool

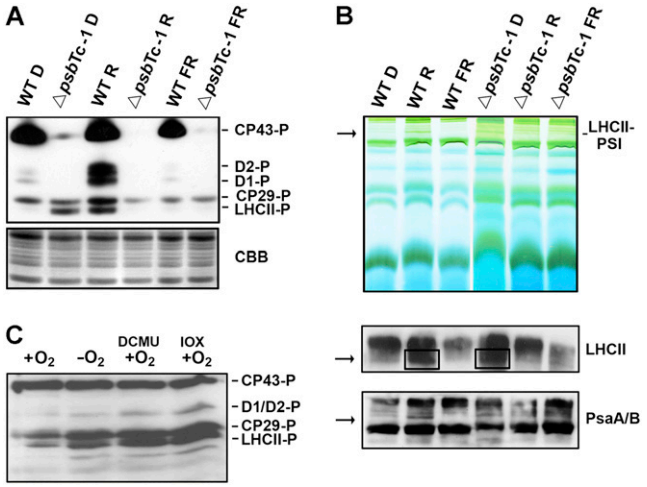

Figure 6. Phosphorylation patterns of PSII proteins and PSI-LHCII association in the wild type (WT) and Δ*psb*Tc-1. A, Phosphorylation analysis of D1/D2, CP43, and LHCII proteins after 24 h of dark adaptation (D), after 20 min of red light illumination (R), and after treatment with far-red light (FR). Phosphorylation was detected with phosphothreonine antibodies. Coomassie Brilliant Blue (CBB) staining is shown as a loading control (bottom). The two independent lines Δ*psb*Tc-2 and Δ*psb*Tc-3 show the same light-dependent phosphorylation pattern (Supplemental Fig. S1C). B, Analysis of protein complexes separated by BN-PAGE in the first dimension (top). Immunoblot analysis of protein complexes separated by BN-PAGE using LHCb1 and PsaA/B antibodies demonstrates the presence of LHCII-PSI supercomplexes (indicated by arrows and boxes) in the wild type under state II conditions and in the mutant after dark adaptation (bottom two panels). C, LHCII phosphorylation after dark incubation of wild-type leaves under aerobic ($+O_2$) and anaerobic ($-O_2$) conditions in the presence and absence of DCMU and Ioxynil (IOX).

(Fig. 6B, top). The composition of the bands representing the LHCII-PSI supercomplex was also demonstrated by immunoblot analysis of the native gel using antibodies raised against LHCII and PsaA/B (Fig. 6B, bottom). These data indicate a role of the PSII protein PsbTc in the oxidation of reduced plastoquinone in the dark.

The Q_B Binding Site Is Required for Oxidation of PQH_2 in the Dark

Reduction of plastoquinone takes place via several nonphotochemical pathways, and reoxidation often depends on oxygen (for review, see Rumeau et al., 2007). A prominent functional effect of the mutation seems to be an alteration in the role of the Q_B binding site important for efficient forward electron flow in the light and presumably reoxidation of the plastoquinone pool, which is nonphotochemically reduced in darkness. Were this true, specific inhibition of the Q_B site with DCMU or Ioxynil in the wild type should prevent plastoquinol oxidation even in the presence of oxygen in the dark. In order to check this assumption, wild-type leaves were first treated with far-red light for 1 h to allow complete oxidation of plastoquinol and dephosphorylation of LHCII (Fig. 6C). Subsequently, leaves were incubated in the dark overnight under aerobic and anaerobic conditions. In the presence of oxygen, LHCII remained in a dephosphorylated state, indicating that plastoquinone remains oxidized. In contrast, in the absence of oxygen, phosphorylation of both LHCII and CP29 was increased, indicative of a reduced plastoquinone pool. DCMU or Ioxynil was added 1 h after far-red light treatment, and leaves were maintained in strict darkness. Indeed, using both inhibitors, LHCII and CP29 were highly phosphorylated after 12 h of dark incubation even under aerobic conditions (Fig. 6C). Since binding of Ioxynil does not change the Q_B site conformation, it is unlikely that phosphorylation of antenna proteins under aerobic conditions is due to structural changes within PSII, allowing easier access of the corresponding kinase(s) to the target. Unlike in Δ*psb*Tc-1, phosphorylation of the PSII proteins CP43, D1, and D2 in the wild type was not affected by treatment with inhibitors. Therefore, we conclude that alterations in the redox regulation of LHC phosphorylation resulted from changes in the Q_B binding site, which is directly and specifically involved in the oxidation of PQH_2 in an oxygen-dependent manner. Accordingly, our data indicate that the presence of PsbTc is directly or indirectly required to keep the Q_B site in proper conformation for the reoxidation of PQH_2.

DISCUSSION

Effect of PsbTc Deletion on Assembly, Stability, and Structure of PSII

Studies on PsbTc deletion mutants were reported from *Synechocystis* 6803 (Iwai et al., 2004) and two *Thermosynechococcus* species (Henmi et al., 2008) representing eubacterial organisms and from *Chlamydomonas reinhardtii* (Monod et al., 1994; Ohnishi and Takahashi, 2001; Ohnishi et al., 2007). Data obtained with *Thermosynechococcus* suggested that PsbTc is involved in the assembly of dimeric PSII complexes. However, since deletion of *psb*Tc in the *Chlamydomonas* mutant resulted only in a weakly impaired PSII, it was concluded that this protein is not essential for the organization and function of PSII. Solubilization studies of proteins labeled in vivo indicate that PsbTc in tobacco is not required for the assembly but rather for the stability of the dimeric PSII core (Fig. 2, B and C).

The absence of PSII-LHCII assemblies in Δ*psb*Tc-1 to -3 is intriguing, since PsbTc has been localized to the region interconnecting PSII monomers next to the central 2-fold axis (Ferreira et al., 2004; Loll et al., 2005). From its outlined function and position, PsbTc could be involved in the attachment of the outer antenna, possibly through interaction with adjacent proteins, like CP47; therefore, it exerts a long-distance effect.

The proposed positions of PsbTc, PsbL, and PsbM close to the central axes of the PSII dimer previously

suggested that these LMW peptides are involved in dimerization (Ferreira et al., 2004; Nield and Barber, 2006). However, PsbI has been shown to represent a component required for the formation of the dimer presumably by forming a "bracket" (Schwenkert et al., 2006), whereas apparently neither PsbTc nor PsbM is essential for PSII dimer assembly. Loss of PsbTc may affect the function and/or conformation of other adjacent proteins, like PsbL. However, Δ*psb*L knockouts are clearly distinct from Δ*psb*Tc plants with respect to photoautotrophic growth, assembly of PSII dimers, photosynthetic performance, and levels of PSII proteins, indicating that neither function nor localization of PsbL is impaired in Δ*psb*Tc knockout plants (Ohad et al., 2004). We cannot rule out that loss of PsbTc causes the removal of PsbM, since the corresponding mutant also shows a 1/5 B band oscillation type and increased LHCII phosphorylation in the dark (Umate et al., 2007). However, phosphorylation of CP43 and recovery of PSII from photoinhibition are not affected in Δ*psb*M, indicating that major deficiencies are due to Δ*psb*Tc inactivation. It is intriguing that specific deletions of the predictably closely located proteins PsbTc, PsbL, and PsbM result in quite diverse phenotypes in higher plants (Ohad et al., 2004; Umate et al., 2007).

Lack of PsbTc Results in Increased D1 Degradation

Increased rates of PSII-mediated plastoquinone reduction exceeding plastoquinol oxidation result in an increased back electron flow and charge recombination, causing damage to PSII core proteins (Keren et al., 1997; Zer and Ohad, 2003; Vass et al., 2007). Only under strong illumination were PSII activity and D1 levels reduced in the *Chlamydomonas* mutant. In contrast to the data obtained with tobacco mutants, photosensitivity and D1 degradation in the presence of CAP were apparently not changed in the *Chlamydomonas* mutant, suggesting that PsbTc may not be relevant for photoprotection but may be required for an efficient recovery of photodamaged PSII in the algae (Ohnishi and Takahashi, 2001). Furthermore, PsbTc appeared to be involved in the activation of forward Q_A electron flow during repair of PSII from photoinhibition in *C. reinhardtii* (Ohnishi et al., 2007). Photosensitivity is more striking with translation inhibitors in Δ*psb*Tc tobacco plants than without. The difference of photoinhibition with and without inhibitors as an indicator of recovery is almost the same in wild-type and mutant plants. This indicates that mutant plants are capable of repair from photoinhibition, although this is delayed compared with that in the wild type, suggesting a similar function of PsbTc in Q_A activation during the repair process in tobacco.

Although the function of PsbTc in different organisms is similar, some species-specific features may reflect adaptations to their ecophysiological niches. Yet, it is conceivable that light sensitivity in tobacco might represent a secondary effect of the mutation, since facilitated back electron flow results in increased rates of charge recombination and related oxidative damage in Δ*psb*Tc.

Effect of PsbTc Deletion on Q_A and Q_B Site Properties and PSII Electron Flow

The conformational changes in the organization of PSII induced by the loss of PsbTc affect Q_A and Q_B site properties and/or interaction, resulting in an increased ratio Q_B/Q_B^- and alterations in the PSII charge recombination, as judged from TL measurements. This indicates that there are more oxidized Q_B sites than semiquinones in the mutant, causing an impaired back electron flow and reduction of the plastoquinone pool in dark-adapted PSII populations. However, it still remains controversial which plastoquinone-binding site is largely or directly affected by the absence of PsbTc, because both peaks of Q and B bands in transformant plants were shifted compared with those of wild-type plants. Due to the closer vicinity of PsbTc to Q_A, it is conceivable that conformational changes at the Q_A site may affect its interaction with the Q_B site. Therefore, the effect on the Q_B site could represent a secondary effect of the mutation, as has also been implied for the long-distance effect on the assembly of PSII-LHCII supercomplexes and the stability of PSII dimers in Δ*psb*Tc.

The increase in the B band emission temperature and the down-shift of the Q band also imply an increase in the redox potential gap between the Q_A/Q_B sites and a decrease of the pheophytin/Q_A redox potential gap, thus lowering the forward electron flow and promoting charge recombination by back electron flow from Q_A. This is supported by a decreased PSII-dependent electron transport capability, measured as oxygen evolution rate, in Δ*psb*Tc to about 72% of wild-type levels.

PsbTc Deletion Alters the Redox State of the Plastoquinone Pool and Phosphorylation of PSII Proteins

It is well established that the association of LHCII, CP26, and CP29 with PSII and partially with PSI (state I and state II, respectively) is regulated via reversible phosphorylation of the chlorophyll *a*/*b*-binding apoproteins (Kargul and Barber, 2008). Activation of the respective kinase(s) is regulated by the interaction of reduced plastoquinone with the oxidation site of the cytochrome b_6f complex (Vener et al., 1997). The orthologous protein kinases, STT7 and STN7 in *Chlamydomonas* and Arabidopsis (*Arabidopsis thaliana*), respectively, are involved in the regulation of phosphorylation of LHCII, CP26, and CP29, although the primary targets of the kinases still remain unknown (Rochaix, 2007).

In this study, it could be shown that accumulation of reduced plastoquinone leads to phosphorylation of LHCII in darkness in Δ*psb*Tc mutant plants. Moreover, BN-PAGE analysis revealed that LHCII is not only phosphorylated but also attached to PSI in dark-

adapted mutant plants. Apparently, no light-induced signals cause migration of the LHCII antenna to PSI in the mutant. Therefore, the data uncover a new level of control of LHCII phosphorylation in darkness.

Although the related protein kinase, STN8, triggers phosphorylation of all three PSII core proteins D1, D2, and CP43 (for review, see Vener, 2006), phosphorylation of D1/D2 proteins is considerably more responsive than that of CP43 to redox regulation in tobacco wild-type plants (Fig. 6A; Umate et al., 2007), indicating that additional kinases could be involved in PSII core protein phosphorylation. Phosphorylation of outer antenna proteins and presumably of PSII core proteins is affected not only by activation/deactivation of the respective protein kinase(s) but also by the exposure of segments of substrates containing phosphorylation sites at thylakoid membrane surfaces and, thus, on their accessibility to the active site of the respective protein kinase(s) (Zer et al., 1999, 2003; Vink et al., 2000). Phosphorylation of the core proteins CP43, D1, and D2 is almost completely abolished in Δ*psb*Tc under all light conditions. The same has been described for Δ*psb*I in tobacco (Schwenkert et al., 2006). As both mutants lack stable PSII-LHCII supercomplexes, it is likely that accessibility for the kinase(s) that phosphorylate PSII core proteins is blocked by structural changes of the PSII dimer in the mutants. In contrast, alterations of phosphorylation patterns of PSII antenna proteins are likely due to physiological consequences rather than structural changes. The effect of PsbTc knockouts on the phosphorylation of PSII core and antenna proteins is unknown from other organisms, and it would be challenging to check whether the lack of PsbTc in *Chlamydomonas* induces similar effects.

Nonphotochemical reduction and reoxidation of plastoquinone takes place via several pathways (for review, see Rumeau et al., 2007). The plastid terminal plastoquinone oxidase has been suggested to be involved in reoxidation of reduced plastoquinone. Alternatively, reoxidation of the PQH_2 pool may be mediated by charge recombination with Q_B and probably subsequently with cytochrome b_{559} (Bondarava et al., 2003). Impaired reoxidation of plastoquinol could account for LHCII phosphorylation in darkness in Δ*psb*Tc plants. Finally, we suggest that PsbTc stabilizes the Q_B binding site in vivo that is essential for oxidation of reduced plastoquinone in darkness in an oxygen-dependent manner, possibly to keep the PSII acceptor side oxidized. Our data indicate that the PSII-dependent oxidation of PQH_2 in darkness predominantly controls the redox state of the plastoquinone pool. Therefore, this effect is prevalent when compared with other activities known to oxidize plastoquinol, like the plastid terminal plastoquinone oxidase localized in stroma lamellae (Rumeau et al., 2007), or with a nonenzymatic PQH_2 oxidation. We postulate that PSII could represent the hitherto unidentified major terminal oxidase involved in chlororespiration in leaves (Nixon, 2000; Bennoun, 2002). A protective role of PSII-mediated oxygen reduction and plastoquinol oxidation in the light-driven electron transport, to avoid overreduction of plastoquinone and harmful charge recombination leading to damage of PSII, remains to be shown.

MATERIALS AND METHODS

Vector Construction and Plant Transformation

The plastid *psb*Tc gene was inactivated by targeted disruption with a selectable terminatorless chimeric *aad*A cassette conferring spectinomycin resistance (Koop et al., 1996). The cassette was inserted in the orientation of the operon (Fig. 1). Using a PCR-based site-directed mutagenesis approach, a diagnostic *Hpa*I restriction site was generated at the 5′ region of *psb*Tc with the oligonucleotides *psb*Tcmut2for (5′-ATCTATGGAAGCATTGGTTAACACATTCCTCTTAGTCTCGAC-3′) and *psb*Tcmut1rev (5′-GTCGAGACTAAGAGGAATGTGTTAACCAATGCTCCATAGAT-3′). The DNA fragment amplified using the oligonucleotides *psb*Tcfor (5′-TTCTACGGCGGTGAACTCAACG-3′) and *psb*Tcrev (5′-TCCTACCGCAGTTCGTCTTGGA-3′) was inserted into a pDrive cloning vector (Qiagen) to produce plasmid p*ΔTc* (Fig. 1A). The chimeric *aad*A gene cassette was excised as a 916-bp *Sma*I-*Hin*dIII fragment, blunted, and ligated into the *Hpa*I site of p*ΔTc*. Tobacco (*Nicotiana tabacum* 'Petit Havanna') plastids were transformed essentially as described (Svab et al., 1990). Selection, culture conditions of the transformed material, and assessment of the homoplastomic state of transformed lines were carried out as described (Swiatek et al., 2003a) using the oligonucleotides 5′-TACTTTGAAATCCGATGGTG-3′ and 5′-CTCCAAAATAATAGATAGAAATACC-3′ (Fig. 1B). All seven independent transformants obtained showed the same phenotype with respect to the F_v/F_m ratio ranging between 0.65 and 0.71. Three lines, Δ*psb*Tc-1 to -3, were selected for further studies on photosynthetic performance, assembly, photosensitivity, and phosphorylation patterns of PSII proteins (Figs. 2–6; Supplemental Fig. S1).

Northern-Blot Analysis

Northern-blot analysis was performed as described (Lezhneva and Meurer, 2004) using either radiolabeled DNA probes or end labeling of specific oligonucleotides with T4 polynucleotide kinase (New England Biolabs). Strand-specific end labeling was performed for *psb*Tc, *psb*H, and *psb*N with the oligonucleotides 5′-GGCGGTTCTCGAAAAAAGATAGCGAAAAAAATTATCCCTAGAGTCGAGACTAAGAGGAATGTATAAACCAATGCTTCCAT-3′, 5′-TTCAATGGTTTTAATAAATCTCCTACCGCAGTTCGTCTTGGACCAGATCTAGAACTGTTTTCAACAGTTTGTGTAGCCAT-3′, and 5′-CTAGTCTCCATGTTCCTCGAATGGATCTCTTAGTTGTTGAGAAGGTTGCCCAAAAGCGGTATATAAGGCGTACCCAGTAA-3′, respectively. The *pet*B and *psb*B probes were amplified with the oligonucleotides 5′-GCATTGTATATTTCCGGAATATGAGTAAAG-3′/5′-CGTTCTTCGAACCAATCATAAACTTTACTC-3′ and 5′-TTGTTCCGGGAGGAATAGCCT-3′/5′-GCCAGTCCAGCACTAACTCTTCG-3′, respectively (Fig. 1C).

Preparation of Thylakoid Membranes, SDS-PAGE, and Immunoblot Analysis

Thylakoid membrane proteins were isolated, separated by SDS-PAGE, and subjected to immunoblot analysis as described (Umate et al., 2007). Quantitative immunoblot analysis was performed using AIDA software (Raytest).

Suc Density Gradients

Thylakoid membrane complexes were separated by Suc gradient centrifugation using 4-week-old in vitro-grown plants (light intensity of 10–20 μE m^{-2} s^{-1}, 12-h photoperiod) as described (Schwenkert et al., 2006).

BN-PAGE

BN-PAGE was performed as described earlier (Schwenkert et al., 2007). Thylakoid fractions were solubilized with either 1% β-dodecylmaltoside or

1.5% digitonin. Lysates were separated on a 4% to 12% polyacrylamide gel. Proteins were either transferred onto polyvinylidene difluoride membranes or gel lanes were excised and run on a second dimension using 15% SDS-PAGE. In vivo labeling was performed using [^{35}S]Met (Schwenkert et al., 2006).

Thylakoid Protein Phosphorylation Assay

State I conditions were adjusted by either keeping plants in darkness for 24 h or treatment with light at 728 nm (PSI light) of 20 μE m^{-2} s^{-1} for 30 min. For state II conditions, leaves were illuminated with light at 650 nm (PSII light) of 45 μE m^{-2} s^{-1} for 30 min. All buffers used for thylakoid preparations contained 10 mM NaF. Phosphorylated proteins were detected using anti-phosphothreonine antiserum (New England Biolabs). Anaerobic conditions were generated by placing leaves in a humid screw-cap vial flushed for 10 min with pure argon at room temperature.

PSII Quantum Yield and Fluorescence Quenching Analysis

A pulse amplitude-modulated fluorimeter (PAM-101; Waltz) was used to study chlorophyll *a* fluorescence kinetics. Leaves dark adapted for not less than 5 min were used for measurements. Red actinic light (650 nm, 5 and 45 μE m^{-2} s^{-1}) was used for measurement of fluorescence parameters. The maximum quantum yield of PSII was determined as $(F_m - F_o)/F_m = F_v/F_m$, and the effective quantum yield of PSII, Φ_{PSII}, was expressed as $F_m' - F_s'/F_m'$ (Genty et al., 1989). qP and NPQ were determined by repetitive saturation pulses. The quenching coefficients, NPQ and qP, were calculated as $(F_m - F_m')/F_m'$ and $(F_m' - F)/(F_m' - F_o)$, respectively (van Kooten and Snel, 1990).

PSI Activity

PSI activity was investigated on leaves as absorption changes of PSI at 830 nm induced by far-red light (ΔA_{max}) and actinic light (ΔA) using the PSI attachment of PAM-101 (Walz). The redox condition of PSI at the indicated light intensities was expressed as the ratio $\Delta A/A_{max}$ (Klughammer and Schreiber, 1994).

Oxygen Evolution Measurements

PSII electron transport activity was determined using a Clark-type oxygen electrode as described (Umate et al., 2007). In order to measure exclusively PSII-dependent electron transport, the PSII-specific electron acceptor *p*-benzoquinone as well as the uncouplers NH_4Cl (5 mM) and gramicidin (3 μM) were used under saturating light conditions. PSII activity of wild-type thylakoids was 198 ± 19 μmol oxygen mg^{-1} chlorophyll h^{-1}.

TL Measurements

TL measurements of thylakoids were measured using a home-built apparatus as described (Schwenkert et al., 2006). The Q band emission resulting from Q_A^-/S_2 charge recombination was measured by blocking electron flow to Q_B with the addition of DCMU (10 μM) or Ioxynil (5, 10, and 20 μM) during dark adaptation. Concentrations of Ioxynil higher than 20 μM were avoided due to high fluorescence quenching induced by this herbicide.

A computer-based simulation program allowing the prediction of S-state ratio and the occupancy ratio Q_B/Q_B^- was employed. The program simulates predicted oscillation profiles and checks for the correlation between simulated and measured values (Umate et al., 2007).

PSII Photoinactivation and Recovery Kinetics

The sensitivity of PSII to oxidative stress was determined using leaf discs of wild-type and Δ*psb*Tc plants exposed to 1,200 μE m^{-2} s^{-1} heterochromatic light. Photoinactivation of PSII was measured as changes in the F_v/F_m parameter as a function of exposure time. To estimate the contribution of the PSII recovery process during treatment with high light, leaf discs were infiltrated with a solution of CAP (200 μg mL^{-1}) in darkness for 30 min prior to exposure to high light. To assess photoinhibition kinetics and capacity to recover PSII activity, leaf discs were exposed in the absence of CAP pretreatment to high light (1,200 μE m^{-2} s^{-1}) until an F_v/F_m of 0.17 was reached in wild-type and Δ*psb*Tc discs and then allowed to recover PSII activity by lowering the light intensity to 3 μE m^{-2} s^{-1} for up to 6 h, measuring the F_v/F_m level every 1 h.

Supplemental Data

The following materials are available in the online version of this article.

Supplemental Figure S1. Studies on the assembly, photoinhibition, and phosphorylation patterns of the independent transformants Δ*psb*Tc-2 and Δ*psb*Tc-3.

Supplemental Figure S2. Separation of wild-type and Δ*psb*Tc-1 thylakoids by BN-SDS-PAGE using 1.5% digitonin.

Supplemental Table S1. Computer-based simulation for the prediction of the S-state ratios and the occupancy ratio Q_B/Q_B^-.

ACKNOWLEDGMENTS

We acknowledge Noam Adir for helpful discussions and Dario Leister for kindly reading the manuscript.

Received July 8, 2008; accepted September 12, 2008; published September 19, 2008.

LITERATURE CITED

Barkan A (1988) Proteins encoded by a complex chloroplast transcription unit are each translated from both monocistronic and polycistronic mRNAs. EMBO J **7:** 2637–2644

Bennoun P (2002) The present model for chlororespiration. Photosynth Res **73:** 273–277

Bondarava N, De Pascalis L, Al-Babili S, Goussias C, Golecki JR, Beyer P, Bock R, Krieger-Liszkay A (2003) Evidence that cytochrome b_{559} mediates the oxidation of reduced plastoquinone in the dark. J Biol Chem **278:** 13554–13560

Cser K, Vass I (2007) Radiative and non-radiative charge recombination pathways in photosystem II studied by thermoluminescence and chlorophyll fluorescence in the cyanobacterium *Synechocystis* 6803. Biochim Biophys Acta **1767:** 233–243

Dekker JP, Boekema EJ (2005) Supramolecular organization of thylakoid membrane proteins in green plants. Biochim Biophys Acta **1706:** 12–39

Ducruet JM, Peeva V, Havaux M (2007) Chlorophyll thermofluorescence and thermoluminescence as complementary tools for the study of temperature stress in plants. Photosynth Res **93:** 159–171

Ferreira KN, Iverson TM, Maghlaoui K, Barber J, Iwata S (2004) Architecture of the photosynthetic oxygen-evolving center. Science **303:** 1831–1837

Genty B, Briantais JM, Baker NR (1989) The relationship between the quantum yield of photosynthetic electron transport and quenching of chlorophyll fluorescence. Biochim Biophys Acta **990:** 87–92

Granvogl B, Zoryan M, Plöscher M, Eichacker LA (2008) Localization of 13 one-helix integral membrane proteins in photosystem II subcomplexes. Anal Biochem (in press)

Hakala M, Tuominen I, Keränen M, Tyystjärvi T, Tyystjärvi E (2005) Evidence for the role of the oxygen-evolving manganese complex in photoinhibition of photosystem II. Biochim Biophys Acta **1706:** 68–80

Haumann M, Liebisch P, Muller C, Barra M, Grabolle M, Dau H (2005) Photosynthetic O_2 formation tracked by time-resolved x-ray experiments. Science **310:** 1019–1021

Henmi T, Iwai M, Ikeuchi M, Kawakami K, Shen JR, Kamiya N (2008) X-ray crystallographic and biochemical characterizations of a mutant photosystem II complex from *Thermosynechococcus vulcanus* with the *psbTc* gene inactivated by an insertion mutation. J Synchrotron Radiat **15:** 304–307

Iwai M, Katoh H, Katayama M, Ikeuchi M (2004) PSII-Tc protein plays an important role in dimerization of photosystem II. Plant Cell Physiol **45:** 1809–1816

Kargul J, Barber J (2008) Photosynthetic acclimation: structural reorganisation of light harvesting antenna: role of redox-dependent phosphorylation of major and minor chlorophyll a/b binding proteins. FEBS J **275:** 1056–1068

Kamiya N, Shen JR (2003) Crystal structure of oxygen evolving photosystem II from *Thermosynechococcus vulcanus* at 3.7-Å resolution. Proc Natl Acad Sci USA **100:** 98–103

Keren N, Berg A, van Kan PJ, Levanon H, Ohad I (1997) Mechanism of photosystem II photoinactivation and D1 protein degradation at low light: the role of back electron flow. Proc Natl Acad Sci USA **94:** 1579–1584

Klughammer C, Schreiber U (1994) An improved method, using saturating light pulses, for the determination of photosystem I quantum yield via $P700^+$-absorbance changes at 830 nm. Planta **192:** 261–268

Kohchi T, Yoshida T, Komano T, Ohyama K (1988) Divergent mRNA transcription in the chloroplast *psb*B operon. EMBO J **7:** 885–891

Koop HU, Steinmüller K, Wagner H, Rossler C, Eibl C, Sacher L (1996) Integration of foreign sequences into the tobacco plastome via polyethylene glycol-mediated protoplast transformation. Planta **199:** 193–201

Krieger-Liszkay A, Rutherford AW (1998) Influence of herbicide binding on the redox potential of the quinone acceptor in photosystem II: relevance to photodamage and phytotoxicity. Biochemistry **37:** 17339–17344

Lezhneva L, Meurer J (2004) The nuclear factor HCF145 affects chloroplast *psa*A-*psa*B-*rps*14 transcript abundance in *Arabidopsis thaliana*. Plant J **38:** 740–753

Loll B, Kern J, Saenger W, Zouni A, Biesiadka J (2005) Towards complete cofactor arrangement in the 3.0 Å resolution structure of photosystem II. Nature **438:** 1040–1044

Minagawa J, Takahashi Y (2004) Structure, function and assembly of photosystem II and its light-larvesting proteins. Photosynth Res **82:** 241–263

Monod C, Takahashi Y, Goldschmidt-Clermont M, Rochaix JD (1994) The chloroplast *ycf8* open reading frame encodes a photosystem II polypeptide which maintains photosynthetic activity under adverse growth conditions. EMBO J **13:** 2747–2754

Müh F, Renger T, Zouni A (2008) Crystal structure of cyanobacterial photosystem II at 3.0 Å resolution: a closer look at the antenna system and the small membrane-intrinsic subunits. Plant Physiol Biochem **46:** 238–264

Nield J, Barber J (2006) Refinement of the structural model for the photosystem II supercomplex of higher plants. Biochim Biophys Acta **1757:** 353–361

Nixon PJ (2000) Chlororespiration. Philos Trans R Soc Lond B Biol Sci **6:** 31–36

Ohad I, Dal Bosco C, Herrmann RG, Meurer J (2004) Photosystem II proteins PsbL and PsbJ regulate electron flow to the plastoquinone pool. Biochemistry **43:** 2297–2308

Ohnishi N, Allakhverdiev SI, Takahashi S, Higashi S, Watanabe M, Nishiyama Y, Murata N (2005) Two-step mechanism of photodamage to photosystem II: step 1 occurs at the oxygen-evolving complex and step 2 occurs at the photochemical reaction center. Biochemistry **44:** 8494–8499

Ohnishi N, Kashino Y, Satoh K, Ozawa S, Takahashi Y (2007) Chloroplast-encoded polypeptide PsbT is involved in the repair of primary electron acceptor Q_A of photosystem II during photoinhibition in *Chlamydomonas reinhardtii*. J Biol Chem **282:** 7107–7115

Ohnishi N, Takahashi Y (2001) PsbT polypeptide is required for efficient repair of photodamaged photosystem II reaction center. J Biol Chem **276:** 33798–33804

Regel RE, Ivleva NB, Zer H, Meurer J, Shestakov SV, Herrmann RG, Pakarasi HB, Ohad I (2001) Deregulation of electron flow within photosystem II in the absence of PsbJ protein. J Biol Chem **276:** 41473–41478

Rochaix JD (2007) Role of thylakoid protein kinases in photosynthetic acclimation. FEBS Lett **58:** 2768–2775

Rumeau D, Peltier G, Cournac L (2007) Chlororespiration and cyclic electron flow around PSI during photosynthesis and plant stress response. Plant Cell Environ **30:** 1041–1051

Rutherford AW, Crofts AR, Inoue Y (1982) Thermoluminescence as a probe of photosystem II photochemistry: the origin of the flash-induced glow peaks. Biochim Biophys Acta **682:** 457–465

Rutherford AW, Govindjee, Inoue Y (1984) Charge accumulation and photochemistry in leaves studied by thermoluminescence and delayed light emission. Proc Natl Acad Sci USA **81:** 1107–1111

Rutherford AW, Krieger-Liszkay A (2001) Herbicide-induced oxidative stress in photosystem II. Trends Biochem Sci **26:** 648–653

Schwenkert S, Legen J, Takami T, Shikanai T, Herrmann RG, Meurer J (2007) Role of the low-molecular-weight subunits PetL, PetG, and PetN in assembly, stability, and dimerization of the cytochrome b_6f complex in tobacco. Plant Physiol **144:** 1924–1935

Schwenkert S, Umate P, Dal Bosco C, Volz S, Mlcòchová L, Zoryan M, Eichacker LA, Ohad I, Herrmann RG, Meurer J (2006) PsbI affects the stability, function and phosphorylation patterns of photosystem II assemblies in tobacco. J Biol Chem **281:** 34227–34238

Shi LX, Schröder WP (2004) The low molecular mass subunits of the photosynthetic supracomplex, photosystem II. Biochim Biophys Acta **1608:** 75–96

Svab Z, Hajdukiewicz P, Maliga P (1990) Stable transformation of plastids in higher plants. Proc Natl Acad Sci USA **87:** 8526–8530

Swiatek M, Greiner S, Kemp S, Drescher A, Koop HU, Herrmann RG, Maier RM (2003a) PCR analysis of pulsed-field gel electrophoresis-purified plastid DNA, a sensitive tool to judge the hetero-/homoplastomic status of plastid transformants. Curr Genet **43:** 45–53

Swiatek M, Kuras R, Sokolenko A, Higgs D, Olive J, Cinque G, Müller B, Eichacker LA, Stern DB, Bassi R, et al (2001) The chloroplast gene *ycf9* encodes a photosystem II (PSII) core subunit, PsbZ, that participates in PSII supramolecular architecture. Plant Cell **13:** 1347–1367

Swiatek M, Regel RE, Meurer J, Wanner G, Pakarasi HB, Ohad I, Herrmann RG (2003b) Effects of selective inactivation of individual genes for low-molecular-mass subunits on the assembly of photosystem II, as revealed by chloroplast transformation: the *psb*EFLJ-operon in *Nicotiana tabacum*. Mol Genet Genomics **268:** 699–710

Takahashi H, Iwai M, Takahashi Y, Minagawa J (2006) Identification of the mobile light-harvesting complex II polypeptides for state transitions in *Chlamydomonas reinhardtii*. Proc Natl Acad Sci USA **103:** 477–482

Thornton LE, Roose JL, Pakrasi HB, Ikeuchi M (2005) The low molecular weight proteins of photosystem II. *In* TJ Wydrzynski, K Satoh, eds, Photosystem II: The Light-Driven Water:Plastoquinone Oxidoreductase. Advances in Photosynthesis and Respiration, Vol 22. Springer, Dordrecht, The Netherlands, pp 121–138

Umate P, Schwenkert S, Karbat I, Dal Bosco C, Mlcòchová L, Volz S, Zer H, Herrmann RG, Ohad I, Meurer J (2007) Deletion of PsbM in tobacco alters the Q_B site properties and the electron flow within photosystem II. J Biol Chem **282:** 9758–9767

van Kooten O, Snel JFH (1990) The use of chlorophyll fluorescence nomenclature in plant stress physiology. Photosynth Res **25:** 147–150

Vass I, Cser K, Cheregi O (2007) Molecular mechanisms of light stress of photosynthesis. Ann N Y Acad Sci **1113:** 114–122

Vener AV (2006) Environmentally modulated phosphorylation and dynamics of proteins in photosynthetic membranes. Biochim Biophys Acta **1767:** 449–457

Vener AV, van Kan PJ, Rich PR, Ohad I, Andersson B (1997) Plastoquinol at the Qo-site of reduced cytochrome *bf* mediates signal transduction between light and protein phosphorylation: thylakoid protein kinase deactivation by a single turnover flash. Proc Natl Acad Sci USA **94:** 1585–1590

Vink M, Zer H, Herrmann RG, Andersson B, Ohad I (2000) Regulation of photosystem II core protein phosphorylation at the substrate level: light induces exposure of the CP43 chlorophyll *a* protein complex to the protein kinase(s). Photosynth Res **64:** 209–221

Wagner D, Przybyla D, Op den Camp R, Kim C, Landgraf F, Lee KP, Würsch M, Laloi C, Nater M, Hideg E, et al (2004) The genetic basis of singlet oxygen-induced stress responses of *Arabidopsis thaliana*. Science **306:** 1183–1185

Westhoff P, Herrmann RG (1988) Complex RNA maturation in chloroplasts: the *psb*B operon from spinach. Eur J Biochem **171:** 51–64

Zer H, Ohad I (2003) Light, redox state, thylakoid-protein phosphorylation and signaling gene expression. Trends Biochem Sci **28:** 467–470

Zer H, Vink M, Keren N, Dilly-Hartwig HG, Paulsen H, Herrmann RG, Andersson B, Ohad I (1999) Regulation of thylakoid protein phosphorylation at the substrate level: reversible light-induced conformational changes expose the phosphorylation site of the light harvesting complex II (LHCII). Proc Natl Acad Sci USA **96:** 8277–8282

Zer H, Vink M, Shochat S, Herrmann RG, Andersson B, Ohad I (2003) Light affects the accessibility of the thylakoid light harvesting complex II (LHCII) phosphorylation site to the protein kinase(s). Biochemistry **42:** 728–738

Zouni A, Witt HT, Kern J, Fromme P, Krauss N, Saenger W, Orth P (2001) Crystal structure of photosystem II from *Synechococcus elongatus* at 3.8 Å resolution. Nature **409:** 739–743